

Anticipating that our target azobispyrrole was likely to be highly coloured, we hypothesised that any such materials formed would be distinguishable, via their optical features, from polypyrroles or dipyrroles such as aza-dipyrins when assessing reaction mixtures using chromatography.^{23,24} Consequently, without delay, yet cognisant that **2** is susceptible to multiple reaction and decomposition pathways, we exposed **2** to the classic conditions used to convert aryl amines into the corresponding diazonium salts (Scheme 1).²⁵ Each step was conducted under an inert atmosphere, and using degassed reagents. Intent on avoiding isolation of the potentially highly reactive dry diazonium salt **3**, the crude reaction mixture was added directly to a coupling solution containing 2,4-diphenyl pyrrole (**4**). Work-up using NH₃ (aq), following a known procedure for azobenzene synthesis,²⁵ did not result in a material with properties suggestive of the desired azobispyrrole **5**. Significant efforts effecting variations in work-up procedures proved equally fruitless. We further noted that after treating **2** with NaNO₂/HCl, the addition of the crude reaction mixture to a coupling solution containing aniline was also unsuccessful in generating any azo compound. However, phenylazopyrrole **7** was obtained upon reversing the roles of the coupling partners (Scheme 1, bottom). This indicates that although the formation and/or productive reaction of the pyrrole diazonium salt **3** is elusive, the reaction of the α -free pyrrole with an aryl diazonium salt provides azo compounds.²⁶

Given that azo coupling, via a pyrrole diazonium salt, was unsuccessful, our attention turned to other synthetic strategies by which azobispyrroles might be isolated. Alternative methods such as oxidative coupling^{27,28} or reactions of diazonium salts with diarylzinc reagents²⁹ were rendered inaccessible due to challenges with the unstable aminopyrrole **2**, despite our best efforts to avoid self-coupling, aza-dipyrin formation and decomposition. Similarly, exploration of a metal-catalysed C–N bond coupling approach involving the reaction of pyrroleboronic acid, phenylpyrroleiodonium compounds and phthalic hydrazide^{30,31} was stymied by our unsuccessful attempts to generate arylpyrroleiodonium triflate salts using methods adapted from work involving phenyl- and mesityl-substituted linear diaryliodonium compounds.^{32,33}

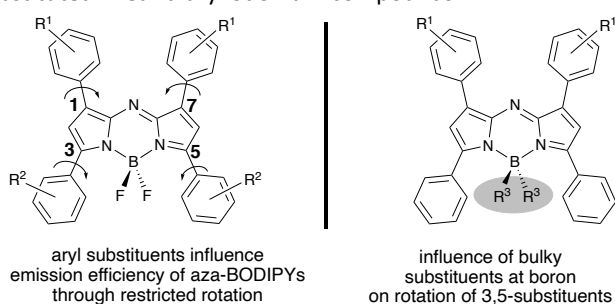


Figure 1: Aryl-substituted aza-BODIPYs

Our ongoing work with aza-BODIPYs includes exploring the photophysical tunability that is achievable by incorporating aryl groups at the boron atom of these dipyrrolic frameworks.³⁴ The ability of substituents at the 3,5- and the 1,7-positions of *F*-aza-BODIPYs to influence the efficiency of emission originates from

the extent to which rotational freedom, and thus nonradiative decay, is restricted as a consequence of either steric bulk or intramolecular interactions (Figure 1, left).³⁵ Although we prepared several arylboryl C-aza-BODIPYs (Figure 1, right), all suffered from negligible fluorescence emission ($\Phi_f < 0.01$). This contrasts with the analogous *F*-aza-BODIPY frameworks wherein B–F...H hydrogen bonds, involving the –BF₂ fragment and the ortho-H atoms of 3- and 5-phenyl groups serve to restrict molecular motion, and consequently, nonradiative decay.³⁵

Hoping to recover aza-dipyrin fluorescence by locking the rotation of the 1,7-substituents, we prepared the nitrobutanone **8a**, bearing a bulky mesityl substituent, and reacted it with NH₄OAc (Figure 2).^{36,35} Reactions of this nature are extensively used for the synthesis of aza-dipyrins, wherein a nitrogen atom occupies the *meso*-position of the dipyrrolic skeleton. A comprehensive study²³ regarding the mechanistic route(s) towards aza-dipyrins concluded that butanones (e.g. **9**, Figure 2) likely form aza-dipyrins (correspondingly, **10**) via reaction of the corresponding α -free pyrrole **D** with the related nitrosopyrrole **E**, both formed in situ, although possibilities for other pathways were also presented. However, an unexpected red spot, appearing on a TLC plate used to monitor the progress of the reaction (Figure 2) between nitrobutanone **8a** with NH₄OAc in ethanol at reflux temperature ((Figure 2), caught our attention.³⁷ Surprisingly, despite employing established conditions, none of the anticipated aza-dipyrin **11a** was isolated. It has been noted that strategies to synthesise aza-dipyrins bearing bulky β -substituents, from appropriately-substituted nitrobutanones, only proceed with low yields, and so the use of glacial acetic acid as an alternative solvent was suggested.³⁵ Accordingly, reaction of **8a** with 35 equiv NH₄OAc in glacial acetic acid enabled isolation of the purple aza-dipyrin **11a** in low yield. In addition, a significant amount of a free-flowing red solid was isolated, and the corresponding characterisation data identified it as the azobispyrrole **13a**.¹⁶ Despite extensive variation of reaction conditions we were unable to augment the yield of **13a** beyond 30%.¹⁶

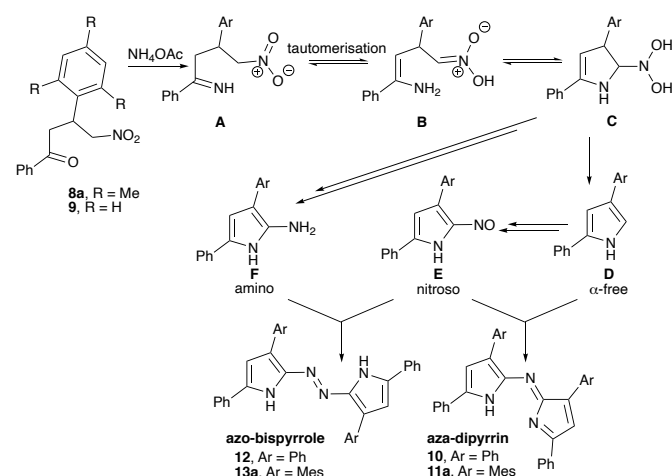
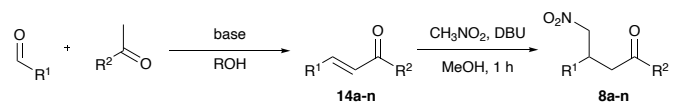


Figure 2: Mechanistic pathways to aza-dipyrin and azo-bispyrrole frameworks

Isolation of the tetra-aryl azobispyrrole **13a** from the reaction mixture prompted an analysis based on mechanistic considerations, cognisant that the formation of aza-dipyrrins from 4-nitro-1,3-diarylbutanones is poorly understood. Insight regarding possible pathways concluded that various routes and rearrangements operate in parallel.²³ Nevertheless, it appears reasonable that a 2,4-diarylpyrrole is formed in situ, and that nitrosation thereof ensues. Reaction of the 2,4-diarylpyrrole with its nitrosated analogue presumably follows, giving rise to aza-dipyrrins.²¹ Presumably, the presence of bulky mesityl groups in 2-phenyl-4-mesitylpyrrole (**D**, Ar = Mes, formed from **8a**) and the nitrosated analogue **E** (Ar = Mes) disfavours condensation between them, rendering alternative outcomes competitive. It also appears reasonable that the corresponding 2-amino pyrrole **F** is formed in situ,²³ and that its reaction with 2-nitroso-5-phenyl-4-mesitylpyrrole (**E**) would, after oxidation, yield the azobispyrrole **13a**. Reaction of **E** and **F** would enable the two mesityl groups to remain more distal to each other than in an aza-dipyrrin. Thus, formation of the azobispyrrole framework likely becomes more competitive as the size of the substituents at the β -position of the constituent pyrroles increases. Nevertheless, the reaction mixture is complex and indeed both **13a** and the aza-dipyrrin **11a** were isolated therefrom.

With the first tetra-aryl azobispyrrole **13a**¹⁶ in hand, complementing the few reported phenylazopyrroles,^{9,26,38} focus moved to assessing the scope for the isolation of systems bearing alternative aryl groups. We were particularly interested in exploring the requirements for steric bulk of the two aryl substituents in analogues of the nitroso- and amino-intermediates **E** and **F**, respectively. A series of chalcones (**14**) were thus prepared via condensation of the appropriate acetophenone and benzaldehyde, as shown in Table 1, and providing a number of novel compounds. These chalcones were then reacted with nitromethane under Michael addition conditions to provide the corresponding nitrobutanones **8b-n**. Reaction of **8b-n** with NH_4OAc was then explored. Given the complexity of the product mixtures, we were gratified to isolate the first series of azobispyrroles, comprising seven additional members (**13b-i**, Figure 3). Intriguingly, aza-dipyrrin **10** was the only product isolated from the reaction of the diphenylated nitrobutanone **8n**, with no trace of the corresponding tetraphenylazobispyrrole apparent on TLC or during work-up. As such, inclusion of a mesityl group or other similarly bulky group at the β -position of the pyrrolic units seems key to promoting azobispyrrole formation in reactions of intermediates of type **E** with those of type **F** (Figure 2). Indeed, reaction of **8i**, to locate a 4-bromo-2-methylphenyl substituent at the β -positions of an azobispyrrole, provided only trace product.

Table 1: Synthesis of chalcones (**14**) and nitrobutanones (**8**)


Entry	R ¹	R ²	Yield 14 (%)	Yield 8 (%)
a	Mes	Ph	90	80
b	(2,6-diCl)C ₆ H ₄	Ph	87	80
c	Mes	(2,5-dimethyl)C ₆ H ₄	78	68
d	Mes	(4-chloro)C ₆ H ₅	94	63
e	(2,6-dichloro)C ₆ H ₄	(4-chloro)C ₆ H ₅	66	89
f	Mes	1-naphthyl	98	77
g	Mes	2-naphthyl	71	80
h	Mes	2-anthracenyl	67	56
i	(4-bromo-2-methyl)C ₆ H ₄	(4-bromo)C ₆ H ₅	86	75
j	Mes	2-thienyl	67	89
k	(2,6-dichloro)C ₆ H ₄	2-thienyl	70	quan.
l	Mes	(4-methoxy)C ₆ H ₄	41	90
m	(2,6-dichloro)C ₆ H ₄	(4-methoxy)C ₆ H ₄	quan.	quan.
n	Ph	Ph	-	79

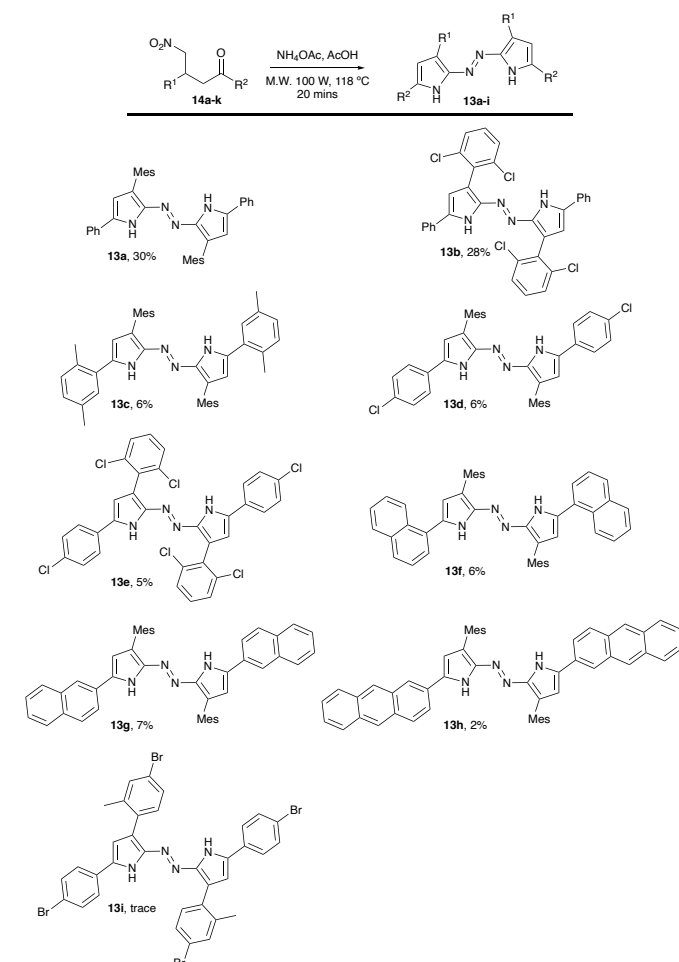


Figure 3. Tetra-aryl azobispyrroles

In contrast, the substituent at the α -position of the pyrrolic units could easily be varied using this synthetic sequence. Phenyl rings bearing alkyl (**13c**) and chloro substituents (**13d-e**)

could be incorporated at the α -position, as could fused aryl groups such as 1- and 2-naphthyl and 2-anthracenyl groups (**13f-h**). In contrast, reactions of nitrobutanones bearing electron-rich substituents (**13j-m**) failed to provide azobispyrroles, perhaps as a consequence of the anticipated enhanced reactivity of the corresponding amino-pyrroles (**F**) bearing α -thienyl and α -anisyl substituents.

Photochemical characterisation of azobispyrroles **13a-h** (Table 2) was then undertaken. In each case, solvent-dependent absorption properties were apparent. With the exception of **13h**, the azobispyrroles were soluble in DMF, MeCN, chloroform, CH_2Cl_2 and acetone, and less soluble in MeOH. Although emission was in all cases negligibly weak, significant Stokes shifts were observed, likely attributable to aggregation or other such structural changes between ground and excited states.^{16,39,40,41} Indeed, more concentrated solutions in MeCN were seen to produce a fine precipitate upon standing.¹⁶ We observed no evidence of *E-Z* switching upon irradiation of these materials; which is unsurprising given the steric encumbrances that would be experienced between mesityl groups in a *Z* configuration.

Table 2. Absorption and emission data for **13a-h**

Entry	Solvent	UV-Vis Absorption Maxima ($\lambda_{\text{max, abs}}$ nm)	Molar Absorptivity ϵ (mol/L cm) $\times 10^4$	Fluorescence Emission ($\lambda_{\text{max, em}}$ nm)	Stokes Shift (nm) ^a
13a	MeCN	504	6.3	602	98
		522	6.3		
	DMF	504	5.1	583	79
		532	5.4	606	
13b	MeCN	500	2.5	601	101
		520	2.3		
	DMF	504	2.1	604	100
		530	2.2		
13c	MeCN	-	-	-	-
	DMF	496	6.2	588	92
13d	MeCN	506	7.1	607	101
		528	7.0		
	DMF	508	5.5	610	102
		538	5.6		
13e	MeCN	500	6.5	606	106
		520	6.4		
	DMF	506	7.1	607	101
		534	7.2		
13f	MeCN	496	2.5	604	108
	DMF	498	2.1	603	105
13g	MeCN	520	2.0	604	84
		544	1.9		
	DMF	522	8.3	605	83
		554	8.2		
13h	MeCN	546	1.5	628	82
		576	1.5		
	DMF	550	0.7	622	72
		584	0.7		

^anegligible; too small for quantum yield (Φ_f) to be accurately calculated

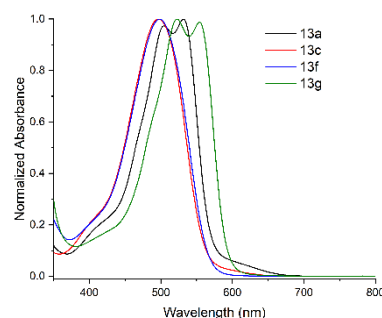


Figure 4: Normalised absorption spectra for **13a**, **13c**, **13f** and **13g** in DMF

Intriguingly, the absorption spectra of most of the azobispyrroles in this series featured two distinct maxima (Figure 4). A solution of **13a** in MeCN was incubated for 1 hour at each of 0 °C and 40 °C and analysed at each temperature, and the dual maxima persisted. However, compounds **13c** and **13f**, whereby the flanking α -aryl substituent imparts greater proximal steric bulk by virtue of the ortho methyl substituent (**13c**) and the position at which the aryl is connected to the pyrrole (**13f**), exhibited a single absorbance maximum (Figure 4). This behaviour is mirrored in the emission profile,

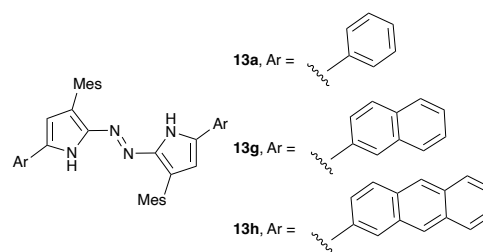


Figure 5. Structural comparison of azobispyrroles **13a**, **13g** and **13h**

notwithstanding the likely contributions of aggregation.¹⁶ As shown in Figure 5, azobispyrroles **13a**, **13g** and **13h** constitute a series with increasingly extended conjugation, courtesy of the arene attached to the α -position of each pyrrole unit via (formal) sequential fusion to additional benzene units. As the size of the π -system increases, a significant red-shift of absorbance is observed (**13a** $\lambda_{\text{max,abs}}$ 504 nm, **13g** $\lambda_{\text{max,abs}}$ 520 nm, **13h** $\lambda_{\text{max,abs}}$ 546 nm; all in MeCN). However, **13f** whereby the α -position of the pyrroles feature 1-naphthyl groups instead of the 2-naphthyl groups of **13g**, retains the absorption characteristics of the phenyl-substituted **13a**. The solid-state structures of **13a**, **13b**, **13f** and **13g** are reported herein (see Supplementary Information for full details). Via single-crystal X-ray diffraction, we observe that in **13g** (and **13a**) the arene at the α -position of the pyrroles makes an angle of $\sim 20^\circ$ with the azobispyrrole core (Figure 6). Meanwhile, the 1-naphthyl substituents of **13f** (Figure 7) deviate distinctly from coplanarity with the pyrrole-N=N-pyrrole core, with an angle of $\sim 40^\circ$ between the planes (Figure 7). Presumably then, the red-shifted absorption characteristics in solution arise from conformations where the terminal aryl group lies closer to coplanarity with the azobispyrrole core, maximising conjugation across the entire chromophore. Furthermore, two polymorphs of **13a** were

obtained: both exhibit comparable characteristics as regards the extent of coplanarity of the flanking phenyl groups and the central core, despite their different crystalline arrangements and solvation states (see Supplementary Information for full details). Coplanarity in these systems is evidently compromised by steric factors and enhanced by hydrogen bonding (see Supplementary Information for full details). The inclusion of solvent (whether water, methanol or chloroform) and the hydrogen bonding it introduces (both as donor and acceptor) must offer more stabilization in the solid-state, promoting non-coplanarity of the terminal aryl groups with the central pyrrole-N=N-pyrrole core, than does the conjugation afforded by the peripheral aromatic groups (whether phenyl or naphthyl) lying in the same plane as the central core. Nevertheless, the different skeletal points by which the naphthyl groups in **13f** and **13g** attach to the pyrrole units clearly affects both the

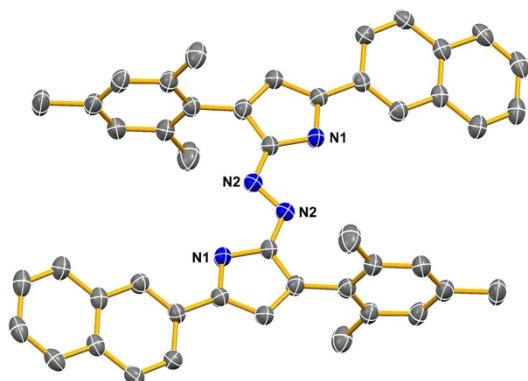


Figure 6: Solid-state structure of α -(2-naphthyl)- β -mesityl azobispyrrole **13g**. Only one half of the molecule is uniquely defined. Three other (half unique) molecules, the solvent molecules and the hydrogen atoms have been removed for clarity. Thermal ellipsoids are drawn at the 50% probability level.

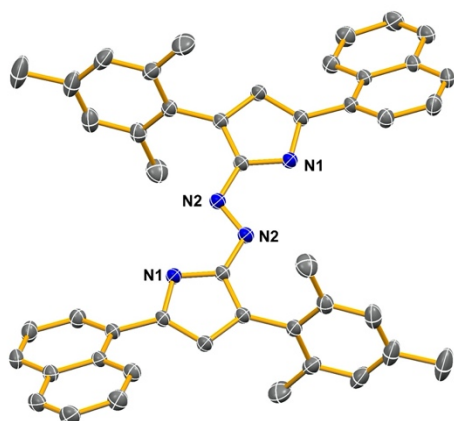


Figure 7: Solid-state structure of α -(1-naphthyl)- β -mesityl azobispyrrole **13f**. Only one half of the molecule is uniquely defined. A second (half unique) molecule, the solvent molecule and the hydrogen atoms have been removed for clarity. Thermal ellipsoids are drawn at the 50% probability level.

photophysical properties in solution, and the solid-state structural features.

Conclusions

The azobispyrrole is emerging as a highly tunable framework, with significant potential for elaboration of the flanking aryl units as a mechanism by which to tune photophysical characteristics. Further modification of optical properties via complexation,¹⁶ utilising the pyrrolic and azo nitrogen atoms, further enables control of photochemical properties by restricting conformational flexibility within the central azobispyrrole unit. Given the wealth of electronic and steric tunability that the pyrrolic construct offers, next steps involve developing synthetic methodologies that enable preparation of azobispyrroles which are not reliant upon the presence of a bulky substituent at the β -positions of the pyrrolic backbone. Identification of a convergent route will enable reactivity, photochemical properties and tunability, and application potential to be fully explored for this promising new heterocycle-containing azo framework.

Author contributions

Conceptualisation: RD-R, SOS and AT

Funding acquisition: AT

Investigation: SOS, RD-R, MA, JWH, AA, RLG, MD, ECS, EBB and KNR

Project administration: AT

Supervision: AT

Writing – original drafts: AT

Writing – review & editing: AT, SOS, RD-R, JWH, AA, RLG, EBB, KNR and AT

Conflicts of interest

There are no conflicts to declare.

Data availability

The data supporting this article have been included as part of the Supplementary Information. Furthermore, crystallographic data for compounds **13a**, **13b**, **13f** and **13g** have been deposited at the CCDC under accession numbers 2449926-27 and 2442944-45 and can be obtained from <https://www.ccdc.cam.ac.uk>.

Acknowledgements

Dr. Michael Lumsden and Mr. Xiao Feng (both at Dalhousie University) are thanked for sharing their expertise in NMR spectroscopy and mass spectrometry, respectively. This research was supported, in part, by: the Canada Research Chairs Program (950-232829); Canada Foundation for Innovation (JELF 39824); Research Nova Scotia (Research Opportunities Fund 2020-1208); Dalhousie University; the Province of Nova Scotia (Nova Scotia Graduate Scholarship to RD-R.); NSERC of Canada via Discovery Grants and the CREATE Training Program in BioActives (510963); and Dalhousie's Southern African Student Education Project (SASEP) scholarship to RLG.

- 1 A. Noble, *Liebigs Ann. Chem.*, 1856, **98**, 253–256.
- 2 A. Bafana, S. S. Devi and T. Chakrabarti, *Environ. Rev.*, 2011, **19**, 350–371.
- 3 B. J. Brüsweiler, S. Küng, D. Bürgi, L. Murali and E. Nyfeler, *RTP*, 2014, **69**, 263–272.
- 4 P. Barciela, A. Perez-Vazquez and M. A. Prieto, *FCT*, 2023, **178**, 113935.
- 5 K. Mezgebe and E. Mulugeta, *RSC Adv.*, 2022, **12**, 25932–25946.
- 6 S. Sahu and S. Kumar Behera, *J. Mat. Chem. C*, 2025, **13**, 3167–3192.
- 7 T. Saßmannshausen, H. Glover, M. Trabuco, W. Neidhart, R. Cheng, M. Hennig, C. Slavov, J. Standfuss and J. Wachtveitl, *J. Am. Chem. Soc.*, 2024, **146**, 32670–32677.
- 8 M. Gupta and Ashy, *Adv. Energy Mater.*, 2024, **14**, 2303845.
- 9 S. Crespi, N. A. Simeth and B. König, *Nat. Rev. Chem.*, 2019, **3**, 133–146.
- 10 Z. Yoshida, H. Hashimoto and S. Yoneda, *J. Chem. Soc. D*, 1971, 1344–1345.
- 11 J. Del Nero and B. Laks, *Synthetic Metals*, 1999, **101**, 440–441.
- 12 G. Zotti, S. Zecchin, G. Schiavon, A. Berlin, G. Pagani, A. Canavesi and G. Casalbore-Miceli, *Synth. Met.*, 1996, **78**, 51–57.
- 13 Y. Wang, J. Ma and Y. Jiang, *J. Phys. Chem. A*, 2005, **109**, 7197–7206.
- 14 P.-O. Åstrand, P. Sommer-Larsen, S. Hvilsted, P. S. Ramanujam, K. L. Bak and S. P. A. Sauer, *Chem. Phys. Lett.*, 2000, **325**, 115–119.
- 15 M. I. Bruce, A. Burgun, M. Jevric, J. C. Morris, B. K. Nicholson, C. R. Parker, N. Scoleri, B. W. Skelton and N. N. Zaitseva, *J. Organomet. Chem.*, 2014, **756**, 68–78.
- 16 Alkaş, Adil; Diaz-Rodriguez, Roberto; Sequiera, Steve; Hilborn, James; Atansi, Mmasinachi; Sullivan, Em; Brown, Emily; Gapare, Rosinah Liandrah; Mutus, Bulent; Robertson, Katherine; Thompson, Alison, *Chem. Commun.*, 2025, in press.
- 17 G. D. Pantoş, M. S. Rodríguez-Morgade, T. Torres, V. M. Lynch and J. L. Sessler, *Chem. Commun.*, 2006, 2132–2134.
- 18 T.-C. Chien, E. A. Meade, J. M. Hinkley and L. B. Townsend, *Org. Lett.*, 2004, **6**, 2857–2859.
- 19 M. A. Marques, R. M. Doss, A. R. Urbach and P. B. Dervan, *Helv. Chem. Acta.*, 2002, **85**, 4485–4517.
- 20 E. B. Brown, R. L. Gapare, J. W. Campbell, A. Alkaş, S. Sequeira, J. W. Hilborn, S. M. Greening, K. N. Robertson and A. Thompson, *Org. Biomol. Chem.*, 2024, **22**, 6122–6128.
- 21 M. A. T. Rogers, *J. Chem. Soc.*, 1943, 590–596.
- 22 C. W. Bird and J. Lu, *Tetrahedron Letters*, 1992, **33**, 7253–7254.
- 23 M. Grossi, A. Palma, S. O. McDonnell, M. J. Hall, D. K. Rai, J. Muldoon and D. F. O'Shea, *J. Org. Chem.*, 2012, **77**, 9304–9312.
- 24 M. J. Hall, S. O. McDonnell, J. Killoran and D. F. O'Shea, *J. Org. Chem.*, 2005, **70**, 5571–5578.
- 25 K.-C. Chang, C.-M. Chu, C.-H. Chang, H.-T. Cheng, S.-C. Hsu, C.-C. Lan, H.-H. Chen, Y.-Y. Peng and J.-M. Yeh, *Polym. Int.*, 2015, **64**, 373–382.
- 26 C. E. Weston, R. D. Richardson, P. R. Haycock, A. J. P. White and M. J. Fuchter, *J. Am. Chem. Soc.*, 2014, **136**, 11878–11881.
- 27 M. Wang, J. Ma, M. Yu, Z. Zhang and F. Wang, *Catal. Sci. Technol.*, 2016, **6**, 1940–1945.
- 28 J.-L. Hu, Y. Wu, Y. Gao, Y. Wang and P. Wang, *ACS Catal.*, 2024, **14**, 5735–5778.
- 29 Z. Duan, S. Dong and J. Li, *Org. Biomol. Chem.*, 2023, **21**, 5506–5510.
- 30 Y. Wang, R. Xie, L. Huang, Y.-N. Tian, S. Lv, X. Kong and S. Li, *Org. Chem. Front.*, 2021, **8**, 5962–5967.
- 31 R. Xie, Y. Xiao, Y. Wang, Z.-W. Xu, N. Tian, S. Li and M.-H. Zeng, *Org. Lett.*, DOI:10.1021/acs.orglett.3c00542.
- 32 M. Reitti, P. Villo and B. Olofsson, *Angew. Chem. Int. Ed.*, 2016, **55**, 8928–8932.
- 33 M. Bielawski, M. Zhu and B. Olofsson, *Adv. Synth. Catal.*, 2007, **349**, 2610–2618.
- 34 R. M. Diaz-Rodriguez, L. Burke, K. N. Robertson and A. Thompson, *Org. Biomol. Chem.*, 2020, **18**, 2139–2147.
- 35 L. Jiao, Y. Wu, Y. Ding, S. Wang, P. Zhang, C. Yu, Y. Wei, X. Mu and E. Hao, *Chem. Asian J.*, 2014, **9**, 805–810.
- 36 Y. Ge and D. F. O'Shea, *Chem. Soc. Rev.*, 2016, **45**, 3846–3864.
- 37 A. Gorman, J. Killoran, C. O'Shea, T. Kenna, W. M. Gallagher and D. F. O'Shea, *J. Am. Chem. Soc.*, 2004, **126**, 10619–10631.
- 38 P. Garg, J. Singh, A. K. Gaur, S. Venkataramani, C. Schäfer and J. George, *Commun. Chem.*, 2025, **8**, 192.
- 39 Z. Liu, Z. Jiang, M. Yan and X. Wang, *Front. Chem.*, 2019, **7**, 712.
- 40 Y. Yang, X. Su, C. N. Carroll and I. Aprahamian, *Chem. Sci.*, 2012, **3**, 610–613.
- 41 K. Tanaka and Y. Chujo, *NPG Asia Mater*, 2015, **7**, e223–e223.